Interface Thickness of a Styrene−Methyl Methacrylate Block Copolymer in the Lamella Phase by Direct Nonradiative Energy Transfer

Yahya Rharbi and Mitchell A. Winnik*

Department of Chemistry, University of Toronto, 80 St. George Street, Toronto, Ontario, Canada M5S 3H6

Received February 13, 2001

ABSTRACT: This paper examines the use of direct nonradiative energy transfer (DET) experiments to determine the interface thickness in films of symmetric poly(styrene-*b*-methyl methacrylate) (PS−PMMA) block copolymers. The films were prepared from mixtures of two polymers of identical length and compositions, labeled at their junctions with either a 9-phenanthryl or 2-anthryl group. The fluorescence decays were analyzed in terms of a model that takes account of the Helfand−Tagami distribution profile of polymer segments at the interface. Reliable data analysis required careful subtraction of a background fluorescence from the measured decay profiles. Unlike neutron reflectivity experiments, DET measurements are insensitive to capillary waves at the interface. This advantage is offset by a strong sensitivity to the characteristic distance for energy transfer R_0, which has to be determined separately. When we take $R_0 = 2.3$ nm, we recover an interface thickness of 4.8 nm. We obtain a theoretical value of 4.2 nm when using the Semenov's finite-chain correction to Helfand−Tagami prediction and the Flory−Huggins χ_{FH} parameter recovered by Russell for partially deuterated d-PS−PMMA copolymer. When we employ the Callaghan and Paul χ_{FH} value for undeuterated PS + PMMA blends, we obtain $\delta = 4.9$ nm.

Introduction

The three major issues of interest in understanding the structure of self-assembling block copolymer melts are the factors that control the shape of the periodic structure, the period length of this structure, and the segment distribution profile (and thickness) of the interface between the two components. Many theoretical studies have focused on the dependence of morphology on the lengths of the component polymer chains and the chemical interaction parameter χ_{FH} between blocks.[1−13] All of these theoretical treatments account for the lamellar structure of symmetric diblock copolymers and predict cylindrical and spherical morphologies for increasingly asymmetric diblock copolymers. Bicontinuous morphologies are sometimes formed by block copolymers at the composition boundary between those that form lamellar and cylindrical structures. These morphologies have been observed directly by electron microscopy.[14] The shape and period length of these structures have also been studied in the bulk state by small-angle scattering experiments using X-rays (SAXS) and neutrons (SANS).[15] Thin films of lamellar block copolymers lend themselves to very detailed examination by specular neutron reflectivity (SNR). SNR measurements provide the most reliable information obtained to date on the thickness of the interface between the two polymers.[16,17]

One of the most investigated diblock copolymers is polystyrene−poly(methyl methacrylate) (PS−PMMA). Russell and co-workers[16,17] have studied thin films of these polymers by SNR and compared the results to SANS experiments on PS + PMMA polymer blends. In the analysis of their SNR experiments on the diblock copolymers, they introduced a theoretical segment density profile based on the theory of Helfand and Tagami (HT)[3−7] and obtained an interface thickness of 5.0 nm. According to theory, the nature of the interface between two homopolymers is very similar to that of the corresponding block copolymer. The description of the block copolymer differs only in an added term for the entropy loss for localization of the junctions in the interface. As a consequence, one can learn a great deal about polymer−polymer interfaces by carrying out SNR measurements on lamellar diblock copolymers and on thin-film sandwiches of the two polymers of interest. Experiments of this sort have been carried out on PS + PMMA by Fernandez et al.[18,19] and by Stamm et al.[20] They reported an interface thickness on the order of 5 nm for polymers with $N\chi_{FH} > 10$.

While the Helfand−Tagami segment density profile is widely accepted, the value of the interface thickness obtained directly from the SNR data ($\delta = 5$ nm) is almost twice the value calculated from the HT model, using the value of χ_{FH} determined by Russell et al.[21] Reflectivity experiments are very sensitive to undulations of the interface and are unable to separate the true thickness of the interface from waviness caused, for example, by the presence of capillary waves. In collaboration with Shull, Russell and co-workers[22] attempted to correct their fitted data for the contribution of capillary waves and revised their value for the PS−PMMA interface to 4 nm for the block copolymers and to 2.9 nm for the blends. Direct evidence of the of the capillary wave contribution was reported by Sferrazza et al.,[23] who examined the ability of a rigid substrate to suppress the undulations due to capillary waves. They examined thin film sandwiches of PS + PMMA blends, in which the thickness of the thin film against the substrate was varied. Indeed, the experimental value of the interface determined by SNR decreased as the polymer films against the substrate became thinner and thinner. From their experiments, they obtained a value for the interface thickness of 2.3 nm.

Our research group has been interested in the use of direct nonradiative energy transfer (DET) measurements as a technique to study interfaces in diblock copolymer micelles and melts.[24,25] These experiments require pairs of diblock copolymers, identical in molecular weight and composition, with a single fluorescent dye attached to the junction between the two components.[24,25] One polymer contains a dye (e.g., phenanthrene, Phe) which can act as a donor (D) in an energy

10.1021/ma010273u CCC: $20.00
Published on Web 06/19/2001

transfer experiment. The other polymer contains a different dye (e.g., anthracene, An), which can act as an acceptor (A) for DET from the donor dye. Because the two block copolymers have the same composition and chain length, their mixtures form the same morphology in the bulk state. This property allows one to carry out a series of experiments at different D/A ratios as a means of evaluating the quality of fit of experimental data to a specific model.

DET experiments take advantage of the distance dependence of the energy transfer rate. The rate of DET between a donor and an acceptor separated by a distance r varies as $(R_0/r)^6$ and is written as[26]

$$w(r,\Omega) = \frac{3}{2}\frac{\kappa^2(\Omega){R_0}^6}{\tau_D r^6} \tag{1}$$

The characteristic (Förster) energy transfer distance R_0 is related to the spectroscopic properties of the donor and acceptor in the medium.

$${R_0}^6 = \frac{2}{3}\frac{9000(\ln 10)\Phi_D}{128\pi^5 n^4 N_A}\int_0^\infty \frac{F_D(\nu)\,\epsilon_A(\nu)}{\nu^4}\,d\nu \tag{2}$$

where N_A is Avogadro's number, Φ_D is the donor fluorescence quantum yield in the absence of acceptor, τ_D is the unquenched donor lifetime, $F_D(\nu)$ is the fluorescence intensity of the donor at the wavenumber ν normalized to unit area on the wavelength scale, and $\epsilon_A(\nu)$ is the extinction coefficient of the acceptor. The term $\kappa^2(\Omega)$ is a geometric orientation factor. We will comment at greater length later in this paper about the determination of R_0 and the influence of the $\kappa^2(\Omega)$ parameter on energy transfer experiments.

In our first publication, we studied several examples of PS−PMMA[24] whose structure at the junction is shown below. These experiments show very clearly that the dyes are concentrated in the interfacial region of the film, with an efficiency of energy transfer much enhanced over that expected for dyes free to explore the entire volume of the sample.

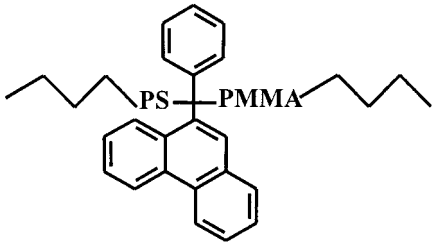

9-phenanthrene-labeled PS-PMMA

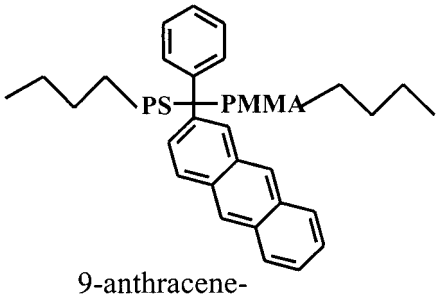

9-anthracene-labeled PS-PMMA

Quantitative information about the thickness of the interface was obtained from the donor fluorescence decay profiles, which were analyzed in terms of a model developed by Klafter and Blumen[27] and adapted to the study of DET in restricted geometries by Klafter, Blumen, and Zumhofen.[28] In this analysis, one fits the donor decay profile to a stretched exponential form appropriate to energy transfer in arbitrary dimensions. In systems of infinite dimensions characterized by self-similarity, the exponent β ($\beta = \Delta/6$) is related to the fractal dimension (Δ) of the lattice. For systems of restricted dimensions, this meaning is lost. The magnitude of β depends only upon edge effects at the boundary of the restricted geometry, and one focuses one's attention on the prefactor P_β, which contains information about the probability of finding an acceptor in a sphere of radius R_0 centered on a donor.

$$I_D(t) = I_0 \exp(-t/\tau_D - P_\beta(t/\tau_D)^\beta) \tag{3}$$

$$P_\beta = \frac{4\pi N_A}{3000}(\gamma_I)^\beta {R_0}^3 \Gamma(1-\beta) C_A \tag{4}$$

In these expressions, I_0 is the intensity at $t = 0$, τ_D is the unquenched donor lifetime, Γ is the gamma function, and γ_I is a preaveraged orientation parameter related to the mean orientation of the transition dipoles.

$$\gamma_I = \frac{3}{2}\langle\kappa^2(\Omega)\rangle \tag{5}$$

In eq 4, C_A is the unknown local concentration of acceptors in the interface. For lamellae, it is related to the known bulk concentration of acceptors $C_{A,0}$ by

$$C_A = \frac{C_{A,0}R_B}{\delta\Phi_B} \tag{6}$$

Information about the interface thickness δ is obtained with the aid of eq 6, in which R_B is the length of the phase made up of the shorter chain and Φ_B is its volume fraction in the sample. Thus, if the period spacing in the sample is known, for example by SAXS measurements, the value of δ can be calculated. Even without this information, the value of δ can be obtained from the ratio δ/R_B using the theory of Ohta and Kawasaki.[29] These experiments yielded a value of the interface thickness about 5 nm.

This analysis does not take into account the detailed shape of the distribution of donors and acceptors (i.e., the junctions) across the block copolymer interface. The most serious consequence of this treatment is that it implicitly assumes a uniform average concentration of acceptors around each donor. Another problem with this analysis is that δ is not defined in a specific way, as it is for example in the theory of Helfand and Tagami. As we shall see below, it is now possible to enter more deeply into the analysis of the donor decay profiles, but in order to do so, one must first carefully subtract background fluorescence from the data. The background signal is due to a weak fluorescence from the polystyrene.

The original theory of energy transfer in restricted geometries of Klafter, Blumen, and Zumhofen[28] was derived only for cases in which all of the donors were related by symmetry. Since all donors are identical, one has only to be concerned with the distribution of

acceptors around a given donor. This feature is implicit in the analysis described above. A more realistic fluorescence model has been developed by Yekta et al.[30] This analysis, which will be described in more detail below, considers the distribution of acceptors around each individual donor and then integrates this response over the distribution of donors in the system. In this way it becomes possible to analyze donor decay profiles in terms of a Helfand−Tagami distribution of junctions across the interface. Simulations show that for lamellar systems one can effectively recover the value of δ from donor decay profiles if the period length of the lamellar spacing is known independently.[31] In the recent past, when we attempted to apply this analysis to experimental data, poor fits were obtained. We now appreciate that the samples we examined had background fluorescence not due to the presence of either dye. This parasitic contribution to the measured signal can be removed, and the corrected data are now able to fit these expressions.

Here we describe the sample preparation, data acquisition, background correction, and data analysis for a sample of PS−PMMA in which the PS block has M_n = 40 000 and the PMMA block has M_n = 41 000, both with a narrow size distribution. This sample was part of the set of PS−PMMA samples examined previously. Using the value of the χ-parameter obtained by Russell,[21] we calculate values of $\chi_{FH}N_{PS} \approx \chi_{FH}N_{PMMA} \approx 15$ and $\chi_{FH}N_{total} \approx 30$, which place this system well outside the weak segregation regime.[32] TEM measurements confirm the lamellar structure, and SAXS measurements in the laboratory of Hashimoto[33] give a period spacing of 36.0 nm. While the DET technique allows one to determine an interface thickness with no major influence due to capillary waves, the magnitude of δ one obtains is very sensitive to the value of R_0, which has to be determined separately. After presenting our results, we examine this sensitivity and the somewhat weaker sensitivity to the orientation parameter $\kappa^2(\Omega)$. We compare the magnitude of the δ we obtain to those obtained from SNR experiments on PS−PMMA block copolymers and blends. This comparison for PS−PMMA is rendered more delicate by the change in the χ-parameter with deuteration of either of the polymer components.

Experimental Section

Materials. The synthesis and characterization of the PS−PMMA samples examined here are described in ref 24. We refer to the phenanthrene-labeled sample as PS−Phe−PMMA, and the anthracene-labeled sample as PS−An−PMMA. Both polymers contain 1.0 chromophores per chain. Using densities of 1.19 for PMMA and 1.04 for PS, we calculate bulk molar concentrations of chromophore (C_D^0,C_A^0) of 1.27 mM for their solvent-free films. For films made up of mixtures of the two polymers, the corresponding donor and acceptor concentrations are calculated as $C_D^0 = f_{phe} \times 1.27$ mM and $C_A^0 = (1 - f_{phe}) \times 1.27$ mM, where f_{phe} is the donor mole fraction in the sample.

Film Preparation. PS−Phe−PMMA (41K/40K) and PS−An−PMMA (40K/41K) copolymers were each dissolved in toluene at 6 wt %. These solutions were mixed to give solutions with f_{phe} = [Phe]/([An] + [Phe]) of 0, 0.05, 0.1, 0.2, 0.3, 0.5, and 1. A gastight syringe was used to measure 0.5 mL ± 3 μL of each solution and spread them onto quartz plates of the same dimensions (2.5 × 2.5 × 0.1 cm). The solutions were then dried very slowly at room temperature, in a box equipped with a small release hole in the presence of a reservoir of toluene in order to minimize the drying rate. After the films were dry (after typically 1 week), the films were annealed at 140 °C for 4 h. Similar methods were used to prepare films of an unlabeled copolymer PS−PMMA (40K/40K) with a very similar molecular weight and composition.

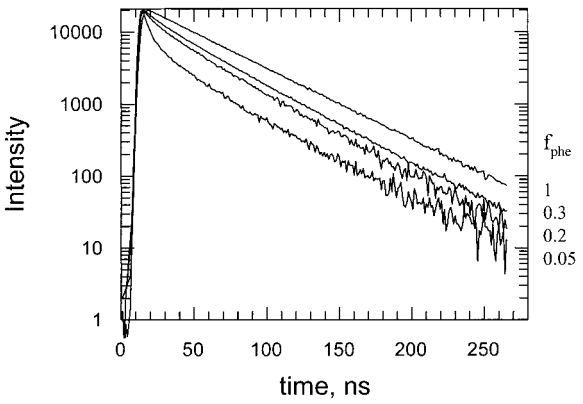

Figure 1. Fluorescence decays from films made of PS−Phe−PMMA (41K/40K) and PS−An−PMMA (40K/41K) copolymers at the molar fraction of Phe-labeled copolymer f_{phe} = 0.1, 0.2, 0.3, and 1. The decays were normalized at their maximum intensities.

Fluorescence Decay Measurements. Fluorescence decay profiles were measured by the single-photon-timing technique at room temperature. The samples were excited at λ_{ex} = 300 nm, and phenanthrene fluorescence was detected at λ_{em} = 350 nm. A band-pass filter (350 ± 5 nm) was used to eliminate all emission from anthracene. The sample holder in the spectrometer was equipped with a goniometer, and the films were positioned at 45° ± 1° from the excitation beam in such a way that the light reflected off the front surface of the film was directed away from the collection optics. Fluorescence was observed through the quartz substrate from the back of the film. The excitation and the emission slits were fully opened for all the measurements, which lasted from 20 to 270 min, according to the concentrations of donor and acceptor in the films.

Results and Discussion

A. Fluorescence Decay Data. 1. Decay Measurements. Figure 1 presents phenanthrene fluorescence decay profiles for films containing various fractions of phenanthrene- and anthracene-labeled copolymer (f_{phe} = [Phe]/([An] + [Phe]) ranging from 0.05 to 1. The decay from the film made of the pure Phe-labeled polymer fits well to an exponential profile with a lifetime of τ_D = 44.4 ns. In the presence of anthracene, the decays deviate from a simple exponential due to DET. For f_{phe} < 0.6, a fast decay appears in the early channels with an apparent lifetime less than 10 ns. This contribution dominates the entire profile for f_{phe} < 0.07. Because the unquenched donor decay is so cleanly exponential, there is a tendency to attribute all deviations from an exponential form to energy transfer. When the fraction of Phe in the sample is small, its emission is weak, both because it competes for light absorption with the anthracene and because energy transfer quenches a substantial fraction of the Phe emission. Under these circumstances, background fluorescence from the polymer itself becomes increasingly important.

We first became aware of this background emission when examining films made of the pure An-labeled copolymer. In these samples, we found a fast decay similar to those observed at short times in samples containing low f_{phe} (Figure 2). In principle, this emission might originate from the An chromophore or from the polymer itself. Anthracene has a finite absorption at the excitation wavelength (300 nm), but its emission ap-

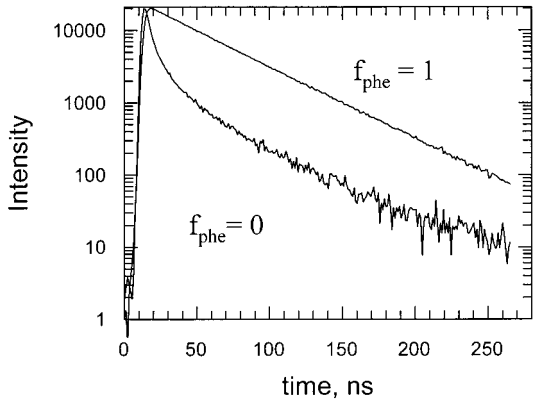

Figure 2. Normalized fluorescence decay curve of a film of PS−An−PMMA (41K/40K) block copolymer compared to that of a film of PS−Phe−PMMA (40K/41K). Both films were excited at 300 nm, and the emission was monitored at 350−355 nm, where no emission from An can be detected.

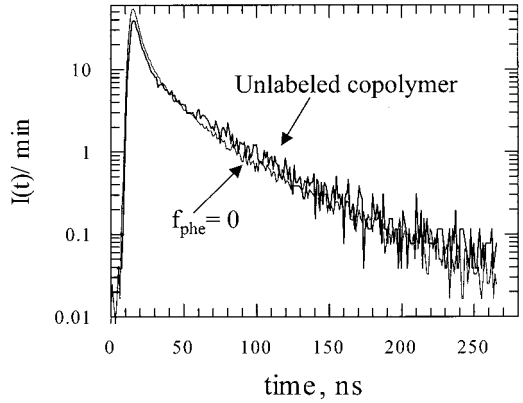

Figure 3. Normalized fluorescence decay curve of a film of PS−An−PMMA (41K/40K) compared to that of film of unlabeled PS−PMMA copolymer.

pears between 350 and 500 nm. Control experiments have shown that our conditions, i.e., excitation at 300 nm and emission at 350 through a band-pass filter (350 ± 5 nm), eliminates more than 95% of the anthracene contribution to the decay. In fact, when we compare decays from the film of pure An-labeled copolymer to that of the unlabeled block copolymer, we found superimposable decays (Figure 3). Thus, we infer that the fast decay is an emission from the polymer itself. The polystyrene portion of the polymer has a very weak absorption tail extending out beyond 300 nm and emission (an excimer emission) between 320 and 400 nm. The contribution of polystyrene emission to the decay depends on the ratio of styrene monomer units to phenanthrene groups and to the relative quantum efficiency of both emissions. For the PS/PMMA polymers examined here, the background emission from the PS component is inconsequential for $f_{phe} > 0.6$. At higher fractions of An, the Phe emission is sufficiently quenched that the background emission becomes important.

2. Background Subtraction. Reliable results in many experimental techniques based upon irradiation, such as neutron- and X-ray scattering, depend on the proper measurement of the background and its subtraction from the signal. Here a similar method must be applied to the fluorescence signal. This correction requires a reference sample, which could be matched to the samples of interest. In these experiments, we can choose either the unlabeled polymer or the pure An-labeled polymer as the reference. To proceed, one must be able to control the thickness and uniformity of the films and the amount of light absorbed by these films during the measurements.

The method of sample preparation employed here requires some technical ability and is described in the Experimental Section. The major technical difficulty is making films that are suitably flat and with similar thickness, ensuring uniform distribution of the material on the quartz plates. Mixed solutions of PS−PMMA containing Phe- and An-labeled block copolymer at 6 wt % in toluene (0.5 mL ± 3 μL) were spread on quartz plates (2.5 cm × 2.5 cm × 1 mm). Fast drying of these solutions resulted in nonuniform films with more material on the edges of the plates. To control the drying rate, the solutions were dried in a closed box with a very small release hole in the presence of a reservoir of toluene. The drying process took a week, resulting in suitably flat and uniform films with similar thicknesses.

To ensure that each polymer film was exposed to a similar light intensity and similar light collection efficiency, fluorescence measurements were carried out in a spectrometer equipped with a goniometer as the sample holder. The films were positioned at 45° ± 1° from the incoming light beam and measured for various amounts of time, ranging from 20 to 270 min. To facilitate sample positioning, measurements were carried out in the open air. Fortunately, the extent of oxygen quenching of the Phe emission in these polymer samples is negligible.

Decay profiles were measured both for donor- and-acceptor-containing films and for films for which only background fluorescence can be detected. The decay representing the background was measured either from the sample made of unlabeled or An-labeled copolymer, since their normalized decays superimpose throughout the time range (Figure 3). The emission intensities were then normalized to the measurement time for the Phe-containing film. It is clear that the background emission contributes an important signal at short times for Phe-containing films at high fractions of An (Figure 4).

The background signal, normalized to equal sample excitation time, was subtracted from the measured sample decay curves. Figure 5 shows semilogarithmic plots of three fluorescence decay curves for samples containing different fractions of Phe-labeled polymer compared to the corresponding background decay. We also show the corrected decay profile after background subtraction. For cases where $f_{phe} > 0.8$, the background contribution to the signal is negligible, and correction for the background is not crucial to the data analysis (Figure 5b). On the other hand, the subtraction technique is reliable only for cases where $f_{phe} > 0.07$, for which the signal-to-background ratio is greater than 10 (Figure 5c). We thus conclude that, with proper attention to sample preparation, it is possible to adapt for DET measurements the same type of background subtraction techniques established for neutron scattering and X-ray scattering experiments.

B. Theoretical Predictions. 1. Donor and Acceptor Distribution across the Interface. The miscibility of the two components of an AB diblock copolymer or a binary A + B polymer blend is determined by the thermodynamics of the polymer−polymer interaction as characterized by the product of their Flory−Huggins parameter χ_{FH} and the polymer chain length N. The polymers we examine (PS−Phe−PMMA and PS−An−PMMA) have $\chi_{FH}N_{total} \approx 30$, which places them in the

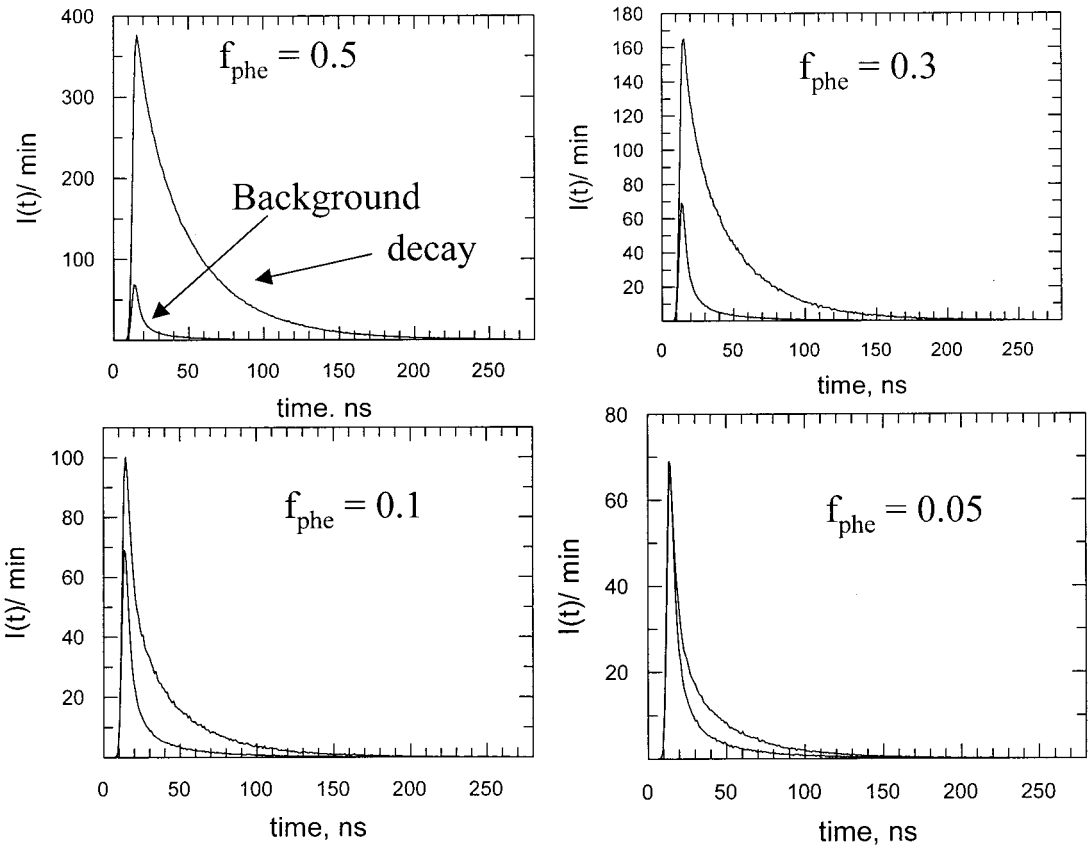

Figure 4. Absolute fluorescence decay curves, plotted linearly against time, for samples made of PS−Phe−PMMA (41K/40K) and PS−An−PMMA (40K/41K) mixtures compared to that of a film of identical thickness made of pure PS−An−PMMA. (a) f_{phe} = 0.5, (b) f_{phe} = 0.3, (c) f_{phe} = 0.1, (d) f_{phe} = 0.05. Optically matched samples were mounted in the goniometer in the sample chamber, and data were collected for identical periods of time.

strong segregation regime ($\chi_{FH}N \gg 10.4$). According to Helfand−Tagami theory, the segment density profiles of PMMA (ρ_{PMMA}) and PS (ρ_{PS}) normal to the interface for strong segregation are given by the expressions[3−7]

$$\rho_{PMMA}(z) = \frac{1 + \tanh(2z/\delta)}{2}$$

$$\rho_{PS}(z) = \frac{1 - \tanh(2z/\delta)}{2} \qquad (7)$$

where δ is the interface thickness. In terms of this model the junction distribution density $P_J(z)$ is given by

$$P_J(z) = \frac{2\pi}{\delta}\,\mathrm{sech}\left(\frac{2z}{\delta}\right) \qquad (8)$$

and the interface thickness δ by

$$\delta_\infty = \frac{2}{(6\chi_{FH})^{1/2}}\left(\frac{d_A b_A^{\,2} + d_B b_B^{\,2}}{2(d_A d_B)^{1/2}}\right)^{1/2} \qquad (9)$$

where d_A, d_B are the monomer densities and b_A, b_B the statistical monomer lengths for PS, b_{PS} = 0.68 nm,[34] and PMMA, b_{PMMA} = 0.74 nm.[35]

While this model is widely accepted for polymer blends, it does not fully describe diblock copolymers. The description of the copolymer differs from the corresponding blend by an added term for the energy penalty for the junction localization. Semenov[36] found that this added term did not affect either the segment density profiles or the junction distribution. He showed that this contribution led to a wider interface thickness for polymers with finite values of $\chi_{FH}N_{total}$.

$$\delta = \delta_\infty + L/(\chi_{FH}N_{total}) \qquad (10a)$$

where L is the lamellae period and δ_∞ is the interface thickness in the limit of high molecular weight (eq 9). When taking into consideration the dependence of L on N_{total} and χ_{FH}, δ becomes

$$\delta = \delta_\infty(1 + 1.34/(\chi_{FH}N_{total})^{1/3}) \qquad (10b)$$

For the case of binary blends, Broseta et al.[37] have taken into account the dependence of the interface thickness δ on the molecular weight

$$\delta = \delta_\infty\left[1 + \ln(2)\left(\frac{1}{\chi_{FH}N_A} + \frac{1}{\chi_{FH}N_B}\right)\right] \qquad (11)$$

where N_A and N_B are the degrees of polymerization of the two components.

The concentration profiles of donor phenanthrene $C_D(z)$ and acceptor anthracene $C_A(z)$ are taken to be proportional to the junction distribution density across the interface (eq 8).

$$C_D(z) = C_D^0 P_J(z)$$

$$C_A(z) = C_A^0 P_J(z) \qquad (12)$$

where C_D^0 and C_A^0 are the bulk molar concentrations of donors and acceptors in the sample.

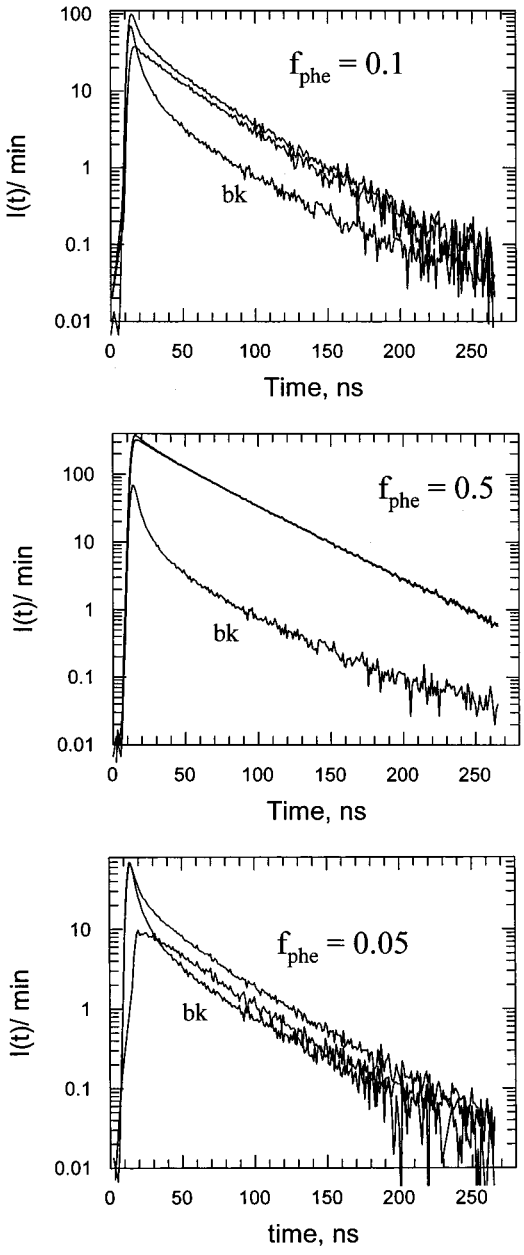

Figure 5. Absolute fluorescence decay curves plotted logarithmically against time for films prepared from a PS−Phe−PMMA (41K/40K) and PS−An−PMMA (40K/41K) mixture at (a) $f_{phe} = 0.1$, (b) $f_{phe} = 0.5$, and (c) $f_{phe} = 0.05$. The y-axis refers to the intensity in counts, divided by the measurement time in minutes. The middle curves are the decay curves after correction by background subtraction. In (c), the background signal-to-noise is too large to obtain meaningful data by background subtraction.

2. Energy Transfer Kinetics Calculation. Nonradiative energy transfer (DET) is commonly used for probing distances in the range 1−10 nm. The rate of DET between a donor and an acceptor separated by a distance r varies as $(R_0/r)^6$ as described in eq 1. In normal practice, the characteristic energy transfer distance R_0 is determined from experiments in fluid solution, where fast molecular rotation (freely rotating dipoles) averages the orientation of each dipole on a time scale faster than the fluorescence decay. Thus, R_0 is calculated using $\langle\kappa^2(\Omega)\rangle = \langle\kappa^2\rangle = {}^2/_3$. This is the origin of the factor ${}^2/_3$ in eq 2. The factor ${}^3/_2\kappa^2(\Omega)$ in eq 1 removes the factor of ${}^2/_3$ in R_0 and introduces the orientation term appropriate for the experiment under consideration.[38] For a given pair of chromophores

$$\kappa^2(\Omega) = \cos^2(\psi)(3\cos^2(\eta) + 1) \tag{13}$$

where η is the angle between the dipole **1** and the vector joining the two dipoles, and ψ is the angle between the dipole **2** and the direction of the electric field at the location of **1**. As eq 1 indicates, for more complex systems, particularly rigid systems, the rate of energy transfer depends on the product of $R_0^6\kappa^2(\Omega)$. The term ${}^3/_2\kappa^2(\Omega)R_0^6$ represents an effective energy transfer distance R_{eff}^6 in the system of interest.

The emission decay of phenanthrene in anthracene-free block copolymer samples is exponential with a lifetime of $\tau_0 = 44.4$ ns. If one had a single distance between donors and acceptors r_{D-A}, the donor fluorescence intensity $I_D(t)$ would be exponential with a rate of $(w(r_{D-A}) + 1/\tau_D)$. This is not the case in our system, which is characterized by a distributions of donors $C_D(z)$ and acceptors $C_A(z)$. Klafter and Blumen have calculated the general form of the donor fluorescence intensity $I_D(t)$ in similar situations (eq 12).[27,28]

$$I_D(t) = \exp(-t/\tau)\int C_D(r)\exp(-\varphi(r,t))\,d\mathbf{r}$$
$$\varphi(r,t) = \int C_A(r'-r)[1-\exp(-w(r')t)]\,d\mathbf{r}' \tag{14}$$

The specific form of $I_D(t)$ for DET between donors and acceptors distributed in planar and spherical geometries was formulated by Yekta et al.[30] Here we use eq 13 developed by Yekta et al. for the planar geometry to model the fluorescence intensity decays in our copolymers.

$$I_D(t) = \exp(-t/\tau_D)\int C_D(z)\exp[-g(z,t)]\,dz$$
$$g(z,t) = 2\pi\int_0^\infty \langle C_A(r,z)\rangle[1-\exp(-tw(r))]r\,dr$$
$$\langle C_A(r,z)\rangle = N_A\int_{z-r}^{z+r} C_A(r')\,dr' \tag{15}$$

We use the H−T profiles to describe the spatial dependence of anthracene $C_A(r)$ and phenanthrene $C_D(r)$ concentrations in this lamella geometry (eq 12).

3. The Orientation Factor. Equation 15 takes into account only the spatial distribution of donors and acceptors. These equations also apply to cases in which it is proper to preaverage the orientation factor. Under these circumstances, eq 1 can be rewritten as

$$w(r) = \langle w(r,\Omega)\rangle = \frac{3}{2}\frac{\langle\kappa^2(\Omega)\rangle}{\tau_D}\left(\frac{R_0}{r}\right)^6 \tag{16}$$

where $\langle\kappa^2(\Omega)\rangle$ is the average of $\kappa^2(\Omega)$. In rigid systems, in which the individual dipoles have orientations that are frozen on a time scale defined by τ_D, one has to examine on a case-by-case basis if preaveraging is justified. More generally, it is $g(z,t)$ that has to be averaged over all possible angular distributions.

$$I_D(t) = \exp(-t/\tau)\int C_D(z)\exp[-g(z,t)]\,dz \tag{17a}$$
$$g(z,t) = 2\pi\int d\Omega\int_0^\infty \langle C_A(r,z)\rangle[1-\exp(-tw(r,\Omega))]r\,dr \tag{17b}$$
$$\langle C_A(r,z)\rangle = N_A\int_{z-r}^{z+r} C_A(r')\,dr' \tag{17c}$$

The evaluation of eq 17 requires knowledge of the angular distribution function $\kappa(\Omega)$ in addition to $C_D(z)$ and $C_A(z)$.

Baumann and Fayer[39] have examined many examples of energy transfer in which preaveraging of the dipole orientation is possible. Preaveraging removes the orientation term to outside the integral in eq 17b to give an expression of the form

$$g(t) = \gamma_I g_0(t) \tag{18}$$

where $g(t)_0$ represents the magnitude of the $g(t)$ function calculated for fast dipole orientation ($\langle\kappa^2\rangle = {}^2/_3$). The nature and magnitude of γ_I depend on geometric details of the examples they considered.

Consider the relatively simple case of uniformly distributed immobile dipoles in the block copolymer interface. In this example, the result of averaging $g(z,t)$ in eq 17 is dependent on the interfacial width δ. For the case of a system characterized by a broad interface, the system is similar to that of donors and acceptors randomly distributed in three dimensions. Baumann and Fayer have shown that in this case

$$\gamma_I = \langle\kappa\rangle/(\langle\kappa^2\rangle)^{1/2} \tag{19}$$

and $\langle\kappa\rangle/(\langle\kappa^2\rangle)^{1/2} = 0.8452$. For a sharp interface, the system is equivalent to that of donors and acceptors distributed in a two-dimensional space. Here Baumann and Fayer have shown that γ_I is given by eq 20, with $\langle\kappa^{2/3}\rangle/(\langle\kappa^2\rangle)^{1/3} = 0.8468$.

$$\gamma_I = \langle\kappa^{2/3}\rangle/(\langle\kappa^2\rangle)^{1/3} \tag{20}$$

Even for a large variation in the interfacial width δ, ranging from 0 to infinity, the $g(t)$ to $g(t)_0$ ratio was found to be almost constant, with γ_I equal to 0.845. It is thus justified, for the case of randomly distributed dipoles, to preaverage $\kappa^2(\Omega)$ in calculating or simulating donor fluorescence intensity decay profiles.

The problem becomes more complicated if the dipoles are preferentially oriented. In block copolymer lamellae, orientation correlation could occur if the direction of the polymer backbone at the junction point has a preferential orientation with respect to the plane of the interface. If the polymer backbone had a preferential orientation, then the transition moment of the chromophores attached to the backbone at the junction point might also have a preferential orientation. In the absence of any evidence for dipole correlation, we proceed with our analysis assuming a preaveraged value of $\kappa^2(\Omega)$ appropriate for randomly oriented immobile dipoles, with $\gamma_I = 0.845$.

4. Simulation Method. Our analysis of the interface thickness for PS−PMMA block copolymers is based upon a comparison of experimental donor decay curves with simulated fluorescence decay profiles $I_{sim}(t)$, in which the interface thickness δ is the only variable to be optimized. We begin by calculating a theoretical intensity profile $I_D(t)$ numerically according to eq 17. In this calculation, we assume a value of the Förster radius R_0 and choose a trial value of the interface thickness δ, introducing the known concentrations of phenanthrene and anthracene and the lamella period. For our sample, the lamellar period spacing is 36 nm as determined in Hashimoto's laboratory by small-angle X-ray scattering.[33] The model intensity profile $I_D(t)$ is

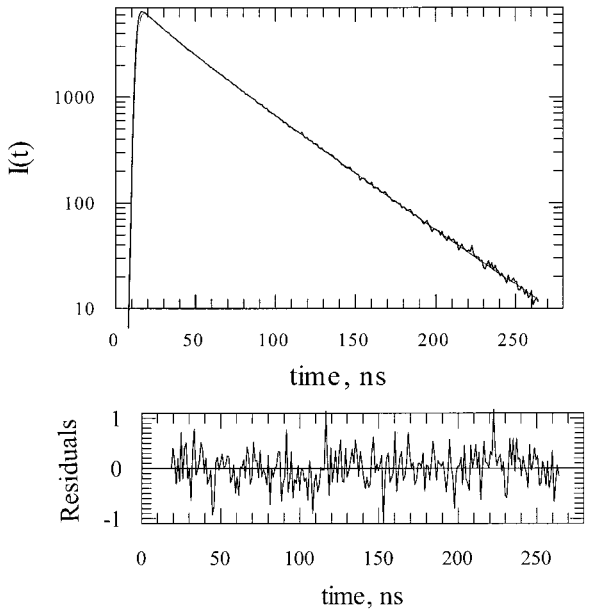

Figure 6. (top) A corrected fluorescence decay for a sample with $f_{phe} = 0.5$ (noise trace), fitted with a model $I_{sim}(t)$ profile calculated from eq 17 (convoluted with the experimental lamp profile). The weighted residuals of the fit are also presented (bottom). The input parameters are $\delta = 5.6$ nm, $R_0 = 2.3$ nm, and $\gamma_I = 1.0$.

then convoluted with the same lamp profile (Lamp(t')) as in the actual experiment for which a comparison will be made.

$$I_{sim}(t) = I_0 \int I_D(t - t')\,\mathrm{Lamp}(t')\,\mathrm{d}t' \tag{21}$$

Subsequently, the experimental decay is fitted to a series of simulated $I_{sim}(t)$ decay profiles in which we recover the intensity at time $t = 0$ (I_0) and calculate the least-squares χ^2 value and the weighted residuals associated with the fit.

B. Interface Thickness Determination. We proceed with our analysis by choosing an R_0 value of 2.3 nm. This R_0 value was determined several years ago by the spectra overlap method, using model compounds and measurements in 1,4-dioxane[40] (eq 2). At about the same time, another student in our group tried to use the spectral overlap method to calculate a value of R_0 in the diblock copolymer itself and obtained a somewhat higher value, 2.4 nm.[24] In retrospect, we suspect that in these experiments background absorption and emission may have contributed to the magnitude calculated for the overlap integral. Until we can develop a more rigorous methodology for determining the magnitude of R_0 in the interfacial domain, we prefer the former value and take it as the starting point for our discussion.

Here we start our analysis by choosing the $R_0 = 2.3$ nm and assuming a freely rotating dipoles $\langle\kappa^2\rangle = {}^2/_3$. Figure 6 shows a normalized experimental donor decay profile, corrected for background fluorescence, fitted to a simulated decay profile based on the Helfand−Tagami model, for various assumed values of δ. The optimum fit is chosen as that in which the weighted residuals are randomly distributed for all the samples investigated. As shown in Figure 7, the optimum fit is obtained for $\delta \approx 5.6$ nm. This value ($\delta = 5.6 \pm 0.5$ nm) is confirmed by the deep minimum in the χ^2 vs δ plot shown in Figure 8.

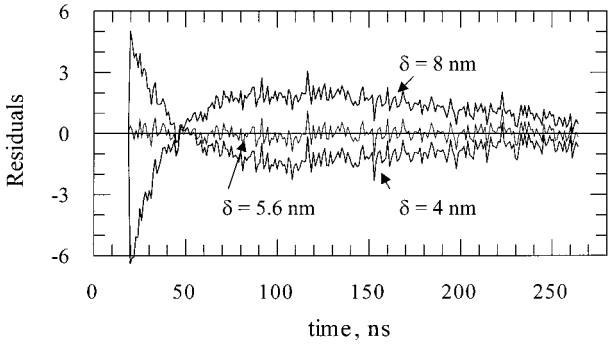

Figure 7. Weighted residuals from fitting the corrected fluorescence decay ($f_{phe} = 0.5$) to the simulated decays for interfacial widths $\delta = 4$, 5.6, and 8 nm. The simulations assume a Förster radius $R_0 = 2.3$ nm and $\gamma_I = 0.845$.

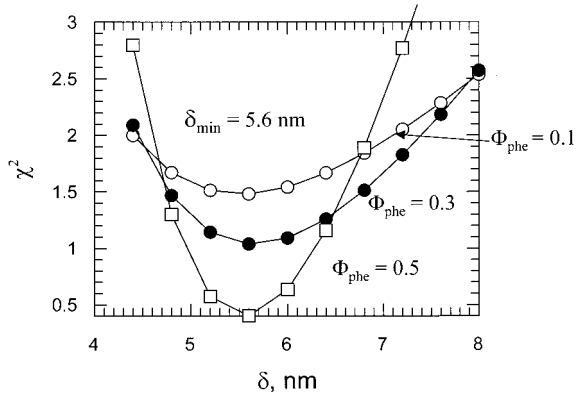

Figure 8. χ^2 surfaces from fits of the corrected fluorescence decay profiles to simulated decay profiles as a function of the assumed interface thickness δ for samples with $f_{phe} = 0.1$, 0.2, and 0.5. The simulations assume a Förster radius $R_0 = 2.3$ nm and $\gamma_I = 0.845$.

Under the condition of our fluorescence measurements, 80 °C below the copolymers T_g, the dipoles are unlikely to be freely rotating as assumed in the previous calculation. When we repeat our analysis by assuming random immobile dipoles, using $R_0 = 2.3$ nm, $\gamma_I = 0.845$, we recover a smaller interface thickness, $\delta = 4.8$ nm.

These values are similar to that calculated previously in our laboratory using samples with high f_{phe} and analyzing the results with the simple restricted geometry model (eqs 3−6). A similar value was obtained from SNR measurements by Russell et al.[16,17] on d-PS/h-PMMA block copolymers and by Stamm et al.[20] and Fernandez et al.[18,19] on h-PS/d-PMMA polymer blends.

These values are significantly larger than those calculated from the theory of polymer interfaces for the limit of high molecular weight (eq 9). With the value of the χ_{FH} parameter reported by Russell et al. in 1990,[21] one calculates $\delta = 2.9$ nm. When using the correction for the finite molecular weight derived by Semenov[36] for block copolymers, we find a broader interface. With the Russell's χ_{FH} value, eq 10a yields $\delta = 4.14$ nm for $L = 36$ nm and eq 10b yields $\delta = 4.22$ nm.

Shull[41] used self-consistent-field calculations to estimate the interface thickness for symmetric PS−PMMA diblock copolymers. He found a similar thickness as that predicted by Semenov in eq 10 for $\chi_{FH}N_{total} \approx 30$, which is the case of our samples. The dissimilarity between the two predictions becomes well pronounced only for $\chi_{FH}N_{total} > 50$, where the SCF calculation yields a much smaller δ than eq 10.

This difference between the results of the neutron reflectivity experiments and the theoretical prediction was discussed in detail by Russell[22] and by Jones.[23] These authors have argued that the SNR technique is sensitive to undulations at the interface resulting from capillary waves. In this way the SNR technique overestimates the interface thickness δ. In the case of the DET experiment, there are three possible causes for the difference between the experimental value of δ and that calculated theoretically: (1) the influence of capillary waves, (2) an error in the DET parameters R_0 and κ^2-(Ω), and (3) problems in the choice of χ_{FH} for calculating the theoretical value of δ.

C. Parameters Affecting the Interface Determination. 1. Capillary Wave Contribution. Neutron reflectivity is the technique of choice for probing interfaces for immiscible polymers and block copolymers. This technique requires flat samples, and the data analysis presumes a flat interface. Any fluctuations due to irregularities in the flatness of the interface, over distances ranging from a few angstroms to a few micrometers, are seen as a broadening of the interfacial thickness. In 1993, the Shull et al.[22] related this discrepancy to capillary waves due to thermal fluctuations at the interface. In the theory of capillary waves, a spectrum of undulations appears at the interface, each with its characteristic wavelength.[42,43] The lower cutoff in the spectrum λ_{min} corresponds to a correlation distance proportional to the interfacial width δ, $\lambda_{min} = c\delta$, where c is a constant ($c \geq 1$). In the limit of a planar surface and small distortions of the interface, the average interface roughness $\langle(\Delta z)^2\rangle$ takes the form

$$\langle(\Delta z)^2\rangle = \frac{k_B T}{2\pi\gamma} \ln\left(\frac{\lambda_{max}}{\lambda_{min}}\right) \tag{22}$$

where γ is the surface tension and k_B is the Boltzmann constant. The lower cutoff λ_{min} and upper cutoff λ_{max} are defined above. In neutron reflectivity, the surface roughness is subtracted in quadratic form from the measured value of the interface thickness.

$$\delta_{app} = [\delta^2 + 2\pi\langle(\Delta z)^2\rangle]^{1/2} \tag{23}$$

where δ_{app} refers to the apparent interface thickness determined in an SNR experiment and δ refers to the true value of the interface thickness.

In the simple case of sandwiched thin polymer films, Shull et al.[22] estimated λ_{max} to be equal to the lateral coherence length of the neutron beam $\lambda_{max} = 1\ \mu$m. They calculated the interface roughness ($\langle 2\pi(\Delta z)^2\rangle^{1/2}$) to be 4.2 nm and an effective interface thickness of 2.9 nm. Because the correlation of the different layers in the block copolymer induces restriction of the surface fluctuation, λ_{max} was chosen to be equal to the lamella period, resulting in an interface roughness of 2.8 nm and an effective interface thickness of 4 nm. Later Sferrazza et al.[23] confirmed experimentally the relevance of capillary waves in neutron reflectivity experiments. They fitted their data to a model describing the dependence of δ_{app} to the thickness of the polymer layer against the rigid substrate. By extrapolating their results to the complete suppression of capillary waves, they obtained a value of δ in good agreement with that predicted by the HT model. This calculation also provides a value for the interfacial tension between PS and PMMA. We note that the value of the interfacial tension

obtained in this way is significantly larger (2.7 vs 1.7 mJ m^{-2}) than its literature value.

The energy transfer experiment loses all sensitivity for donor−acceptor pairs separated by as much as $2R_0$. For the Phe−An pair, the maximum distance sensitivity is on the order of 4 nm, which is in the same range as the minimum cutoff $\lambda_{min} = c\delta$, for the extreme case of $c \approx 1$. When one considers energy transfer in a small slice through a lamellar sample, for a section on the order of 4 nm thick, capillary waves have no major effect on the extent of energy transfer. One should note that this conclusion applies to the specific case of donors and acceptors covalently bound to the block copolymer junctions. For the case of donors and acceptors randomly distributed in the two components of a polymer blend confined in a sandwich geometry, capillary waves can affect the extent of energy transfer by increasing the interfacial area between the donor- and acceptor-labeled domains.

2. The Choice of the χ_{FH} Parameter. In 1990, Russell et al.[21] reported their studies of the chemical interaction parameter χ_{FH} between PS and PMMA based upon neutron scattering measurements in a system of low molecular weight block copolymers d-PS/h-PMMA. For this type of experiment, the data analysis invokes the random-phase approximation, and the authors obtained $\chi_{FH} = 0.028 + 3.9/T$.[21] In 1993, Callaghan and Paul[44] described cloud point measurements on blends of h-PS and h-PMMA. They reported a smaller χ_{FH} value at normal experimental temperatures and a somewhat weaker temperature dependence ($\chi_{FH} = 0.021 + 3.20/T$). They suggested that the difference in the two sets of results might be due to an isotope effect on the χ_{FH} parameter. There is support in the older literature for this point of view.[45] Russell[46] followed up this suggestion by publishing his neutron scattering data on other low molecular weight PS−PMMA copolymers h-PS/d-PMMA, d-PS/h-PMMA, and d-PS/d-PMMA. He confirmed that the magnitude of the χ_{FH} parameter depends on which block is deuterated. All three of his samples exhibited the same temperature dependence of χ_{FH}.

These results are important to us in two respects. First, they indicate that we have to take the effect of deuteration into account when we choose a χ_{FH} parameter for the calculation of a theoretical value of the interface thickness. Second, when we compare our values for δ with those obtained by SNR, we have to take account of the effect of deuteration on δ arising from its influence on χ_{FH}. Kressler et al.[47] have commented extensively on the difficulty in obtaining a unique value of χ_{FH} for PS and PMMA, even apart from the issue of isotope effect.

If we assume that the small dye content in our samples (0.12 mol %) does not affect the interaction between PS and PMMA, then the chemical interaction between the polymers blocks is most likely to be comparable to that reported by Callaghan and Paul.[44] As reported above, changing the fraction of phenanthrene and anthracene in the films does not affect the recovered interface thickness. This can be seen as a partial confirmation that the idea that one Phe or An group at the junction is unlikely to alter the PS/PMMA interaction. One should recall that "normal" unlabeled samples of PS−PMMA contain two phenyl groups at the junction from the use of 1,1-diphenyl ethylene as a switching group in the block copolymer synthesis. When we calculate the interface thickness using eq 9, the Callaghan and Paul value χ_{FH} for 140 °C (our sample annealing temperature), and the Semenov correction (eq 10a) for finite chain length of the block copolymer, we obtain an interface thickness $\delta = 4.9$ nm. This value is similar to that ($\delta = 4.8$ nm) recovered from our DET experiments, using $R_0 = 2.3$ nm and $\gamma_I = 0.845$.

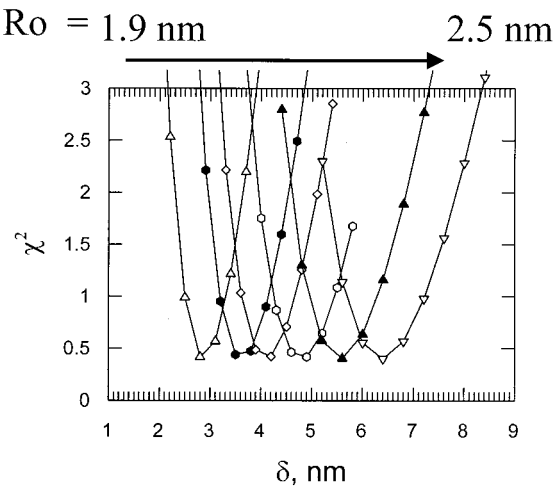

Figure 9. χ^2 surfaces from fits of the corrected fluorescence decay profiles ($f_{phe} = 0.5$) to simulated decay profiles as a function of the assumed interface thickness for various R_0 values ranging from 1.9 to 2.5 nm and $\gamma_I = 0.845$.

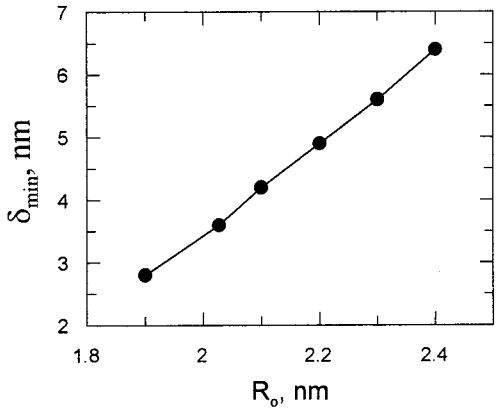

Figure 10. Plot of the "best-fit" interface thickness values δ, taken from the minima in the χ^2 vs δ plots in Figure 9, as a function of the assumed values of R_0.

3. Dependence on R_0. The rate of energy transfer $w(r)$ varies as R_0^6 (eq 16). Values of R_0^6 are determined directly by the spectral overlap method. Nevertheless, small errors in R_0 can lead to significant errors in the determination of δ. To test this idea, we carried out a series of simulations using various assumed values of R_0. For each R_0 value, we examined the dependence of the quality of the fit (χ^2) for an experimental decay curve on the chosen value of δ. These results are shown in Figure 9. The same minimum value of χ^2 (0.5) is found for the different fits, leading to the conclusion that all of the R_0 values, and their corresponding δ values, are possible solutions to the curve-fitting problem. We show in Figure 10 that a variation in R_0 from 1.9 to 2.4 nm leads to a variation in the recovered value of δ from 2.7 to 6.5 nm. Thus, to determine an accurate value of δ, the Förster radius R_0 must be known precisely (and accurately) from independent experiments.

Even though the plot in Figure 10 demonstrates that the calculated of δ is very sensitive to the value of R_0

used in the calculation, values of R_0 can be determined with excellent precision. When one employs the spectral overlap method as described in eq 2, one can determine R_0^6 to a precision of ca. ±10%. Thus, the random error in an R_0 value of 2.3 nm is ca. ±0.05 nm. This level of uncertainty contributes an uncertainty of about 0.5 nm to the calculated value of δ. If one combines the errors associated with fitting the data as shown in Figure 8 with a 0.05 nm uncertainty in R_0, the uncertainty in the recovered value of δ somewhat less than 1 nm, a precision comparable to that obtained in SNR experiments.[48]

A complicating feature of the determination of R_0 by the spectral overlap method is that spectral shifts between fluid solution and polymer films can lead to changes in the overlap integral which are hard to determine. An alternative approach to determining R_0 is to carry out fluorescence decay measurements directly in polymer matrices, using model compounds for the dye, or dye-containing oligomers, where one can safely assume that the dyes are randomly distributed in three dimensions. Individual decay curves can be fitted to eq 3 for various donor−acceptor concentrations. In this way, the value of P_β (eq 4), which is proportional to R_0^3, can be evaluated with a precision of about 5%. This approach leads to a similar precision in R_0. Future experiments of this type will help to define the value of R_0 appropriate for the specific experiments described here.

There are other much more subtle problems associated with correlation effects that might enter into the DET determination of the interface thickness. For example, correlation hole[49] effects could perturb the junction distribution, and this in turn would lead to a lower efficiency of energy transfer than that predicted by a random spatial distribution of dyes. There is also the possibility that correlations among the backbone vectors at the junctions could affect the orientation of the transition dipoles of the chromophores. This factor would affect the magnitude of the orientation term $\kappa^2(\Omega)$. Neither topic has been addressed theoretically. If theoretical calculations were to indicate that these effects are important, DET experiments on diblock copolymers with appropriately chosen chromophores at the junction should be able to test these ideas.

In conclusion, we have described DET experiments on junction-labeled block copolymers and discussed how the data can be analyzed to obtain values of the interface thickness. Before fitting the raw data to models, they have to be corrected for a weak background fluorescence. To obtain optimum values of the interface thickness δ, the corrected donor fluorescence decay profiles were fitted to simulated fluorescence decay curves in which δ was the only adjustable parameter. The simulations assumed a Helfand−Tagami junction distribution profile at the PS−PMMA interface. The recovered value of the interface thickness δ was found to be free of any complications caused by capillary waves but very sensitive to the value of the characteristic energy transfer distance R_0. Assuming an R_0 value of 2.3 nm and an orientation parameter characteristic of random immobile transition moments, the interface thickness was found to be 4.8 nm. We obtain a theoretical value of 4.2 nm when using the Semenov's finite-chain correction to the Helfand−Tagami prediction and the Flory−Huggins χ_{FH} parameter recovered by Russell for partially deuterated d-PS−PMMA copolymer. When we employ the Callaghan and Paul χ_{FH} value for undeuterated PS + PMMA blends, we obtain $\delta = 4.9$ nm.

Acknowledgment. The authors thank NSERC Canada for their support of this research. M.A.W. thanks the Canada Council for a Killam Fellowship.

References and Notes

(1) Meier, D. J. *J. Polym. Sci., Part C* **1969**, *26*, 81.
(2) Leary, D. J.; Williams, M. C. *J. Polym. Sci., Part B* **1970**, *8*, 335. (b) *J. Polym. Sci., Polym. Phys. Ed.* **1973**, *11*, 345.
(3) Helfand, E.; Tagami, Y. *J. Chem. Sci., Part B: Polym. Lett.* **1971**, *9*, 741.
(4) Helfand, E.; Tagami, Y. *J. Polym. Sci., Part B* **1971**, *9*, 741.
(5) Helfand, E.; Sapce, A. M. *J. Chem. Phys.* **1975**, *62*, 1327.
(6) Helfand, E. *Macromolecules* **1975**, *8*, 552.
(7) Helfand, E.; Wasserman, Z. R. *Macromolecules* **1980**, *13*, 994.
(8) Leibler, L. *Macromolecules* **1980**, *13*, 1602.
(9) Milner, S. T. *Science* **1991**, *251*, 905.
(10) Helfand, E. *Macromolecules* **1992**, *25*, 492.
(11) Zhulina, E. B.; Borisov, O. V. *J. Colloid Interface Sci.* **1990**, *137*, 495; **1990**, *144*, 507.
(12) Olvera de la Cruz, M. *Phys. Rev. Lett.* **1991**, *67*, 85.
(13) Vavasour, J. D.; Whitmore, M. D. *Macromolecules* **1992**, *25*, 5477.
(14) Hashimoto, T.; Fujimura, M.; Kawai, H. *Macromolecules* **1980**, *13*, 1660.
(15) Bates, F.; Fredrickson, G. H. *Annu. Rev. Phys. Chem.* **1990**, *41*, 525.
(16) Anastasiadis, S. H.; Russell, T. P.; Satija, S. K.; Majkrzak, C. F. *J. Chem. Phys.* **1990**, *92*, 5477.
(17) Russell, T. P.; Menelle, A.; Hamilton, W. A.; Smith, G. S.; Satija, S. K.; Majkrzak, C. F. *Macromolecules* **1991**, *24*, 5721.
(18) Fernandez, M. L.; Higgins, J. S.; Penfold, J.; Ward, R. C.; Schackleton, C.; Walsh, D. J. *Polymer* **1988**, *29*, 1923.
(19) As pointed out in ref 21, the authors in ref 18 calculated the interface thickness in terms of Debye−Waller factor in the reflectivity equation, which yielded a value of 2 nm. The correct value in the real space should be higher by a factor of $(2\pi)^{1/2}$, $\delta = 5$ nm.
(20) Schubert, A. W.; Stamm, M. *Europhys. Lett.* **1996**, *35*, 419.
(21) Russell, T. P.; Helm, R. P.; Seeger, P. A. *Macromolecules* **1990**, *23*, 890.
(22) Shull, K. R.; Mayes, A. M.; Russell, T. P. *Macromolecules* **1993**, *26*, 3929.
(23) Sferrazza, M.; Xiao, C.; Jones, R. A. L.; Bucknall, D. G.; Webster, J.; Penfold, J. *Phys. Rev. Lett.* **1997**, *78*, 3693.
(24) Ni, S.; Zhang, P.; Wang, Y.; Winnik, M. A. *Macromolecules* **1994**, *27*, 5742.
(25) Tcherkasskaya, O.; Spiro, J. G.; Ni, S.; Winnik, M. A. *J. Phys. Chem.* **1996**, *100*, 7114. (b) Tcherkasskaya, O.; Ni, S.; Winnik, M. A. *Macromolecules* **1996**, *29*, 4241.
(26) Lakowicz, J. R., Ed.; *Principles of Fluorescence Spectroscopy*; Plenum Press: New York, 1983; Vol. 10.
(27) Klafter, J. M.; Blumen, A. *J. Chem. Phys.* **1984**, *80*, 875.
(28) Klafter, J. M.; Blumen, A.; Zumhofen, G. *J. Chem. Phys.* **1986**, *85*, 4087.
(29) Ohta, T.; Kawasaki, K. *Macromolecules* **1986**, *19*, 2621. (b) Kawasaki, K.; Ohta, T.; Kohrogui, M. *Macromolecules* **1988**, *21* 2972.
(30) Yekta, A.; Duhamel, J.; Winnik, M. A. *Chem. Phys. Lett.* **1995**, *235*, 119. (b) Yekta, A.; Winnik, M. A.; Farinha, J. P. S.; Martinho, J. M. G. *J. Phys Chem A* **1997**, *101*, 1787.
(31) Yekta, A.; Spiro, J. G.; Winnik, M. A. *J. Phys. Chem. B* **1998**, *102*, 7960.
(32) Frederickson, G. H.; Helfand, E. *J. Chem. Phys.* **1987**, *87*, 697.
(33) Hashimoto, T.; Sakamoto, N. Unpublished results.
(34) Ballard, D. G. H.; Wignall, G. D.; Schelten, J. *Eur. Polym. J.* **1973**, *9*, 965.
(35) Kirste, R. G.; Kratky, O. *Z. Phys. Chem.* **1962**, *31*, 383. (b) Kirste, R. G. *Makromol. Chem.* **1967**, *101*, 91.
(36) Semenov, A. N. *Macromolecules* **1993**, *26*, 6617.
(37) Broseta, D.; Frederickson, G. H.; Helfand, E.; Leibler, L. *Macromolecules* **1990**, *23*, 132.
(38) Steinburg, Z. I. *J. Chem. Phys.* **1968**, *48*, 2411.
(39) Baumann, J.; Fayer, M. D. *J. Chem. Phys.* **1986**, *85*, 4087.
(40) Duhamel, J.; Yekta, A.; Ni, S.; Khaykin, Y.; Winnik, M. A. *Macromolecules* **1993**, *26*, 6255.

(41) Shull, K. R. *Macromolecules* **1992**, *25*, 2122.
(42) Lacasse, M. D.; Grest, G. S.; Levine, A. J. *Phys. Rev. Lett.* **1998**, *80*, 309.
(43) Buff, P. F.; Lovett, R. A.; Stillinger, F. H. *Phys. Rev. Lett.* **1965**, *15*, 621.
(44) Callaghan, T. A.; Paul, D. R. *Macromolecules* **1993**, *26*, 2439.
(45) Lin, J.; Roe, R. *Macromolecules* **1987**, *20*, 2168. (b) Atkin, A. L.; Kleintjens, L. A.; Koningsveld, R.; Fetters, L. J. *Polym. Bull.* **1982**, *9*, 347.
(46) Russell, T. A. *Macromolecules* **1993**, *26*, 5819.
(47) Kressler, J.; Higashida, N.; Shimomai, K.; Inoue, T.; Ougizawa, T. *Macromolecules* **1994**, *27*, 2448.
(48) For the neutron reflectivity experiments reported for PS/PMMA blends and PS−PMMA diblock copolymers, the value of the apparent interface thickness before correcting for capillary wave is approximately 5.0 ± 1.0 nm. If we use a more optimistic value of 0.8 nm as suggested by the data in Sferrazza et al.[23] and take the capillary wave contribution to be exactly 2.8 nm for the diblock copolymer, we calculate $\delta = 4.3 \pm 0.8$ nm.
(49) Mendelsohn, A. S.; Delacruz, M. O.; Torkelson, J. M. *Macromolecules* **1993**, *26*, 6789.

MA010273U